Ocean acoustic hurricane classification

Joshua D. Wilson and Nicholas C. Makris
Massachusetts Institute of Technology, Cambridge, Massachusetts 02139

(Received 18 August 2005; accepted 7 October 2005)

Theoretical and empirical evidence are combined to show that underwater acoustic sensing techniques may be valuable for measuring the wind speed and determining the destructive power of a hurricane. This is done by first developing a model for the acoustic intensity and mutual intensity in an ocean waveguide due to a hurricane and then determining the relationship between local wind speed and underwater acoustic intensity. From this it is shown that it should be feasible to accurately measure the local wind speed and classify the destructive power of a hurricane if its eye wall passes directly over a single underwater acoustic sensor. The potential advantages and disadvantages of the proposed acoustic method are weighed against those of currently employed techniques. © *2006 Acoustical Society of America.* [DOI: 10.1121/1.2130961]

PACS number(s): 43.30.Nb, 43.30.Pc [ADP] Pages: 168–181

I. INTRODUCTION

A case is made that it may be practical to safely and inexpensively determine local wind speed and classify the destructive power of a hurricane by measuring its underwater acoustic noise intensity. Sea-surface agitation from the action of wind and waves is a dominant source of ambient noise in the ocean.[1,2] This noise can be described as a sum of fields radiated from many random sources on the sea surface.[3–8] If the surface noise sources have the same statistical distribution, Ingenito and Wolf have shown that wind-generated noise spectral intensity is the product of two separate factors, a waveguide propagation factor and a "universal ambient noise"[9] source factor which is a function of wind speed but otherwise is expected to be effectively independent of horizontal position.

The concept of using underwater sound to estimate wind speed was first considered by Shaw *et al.*[10] for spatially uniform wind speed distributions. They found sound pressure level in dB to be linearly related to the log of the wind speed. The idea of a universal ambient noise source factor was implicit in their approach. We will show that the slope of their linear relationship corresponds to the universal ambient noise factor and the intercept to the waveguide propagation factor. Evans *et al.* demonstrated that these estimates could be made to within ±1 m/s in the 5 to 10 m/s wind speed range,[11] which is much less than hurricane wind speeds.

Many experiments have been conducted to determine the relationship between local wind speed and underwater noise intensity as noted in Ref. 12. A common difficulty in these experiments has been contamination from shipping noise.[12,13] This typically leads to poorer correlation and greater variance in estimates of the relationship between wind speed and noise intensity.[12] Two experimental studies conducted over many months that minimized this contamination show that a consistent high-correlation power-law relationship exists.[11,14] They also show underwater noise intensity to be linearly proportional to wind speed to a frequency-dependent power, ranging from two to four, for wind speeds between 5 and 20 m/s. While no measured data have been published relating ambient noise and wind speed in a hurricane, the only known mechanism that would cause a roll-off in the extrapolation of these power laws is attenuation by bubbles.[15] This attenuation, however, is insignificant at low frequencies and can be accurately measured and modeled at high frequencies.

We find that it may be possible to estimate local hurricane wind speed by generalizing the approach of Shaw *et al.*[10] We show that the wind-generated noise received by a single underwater acoustic sensor in a hurricane can be well approximated by sea-surface contributions so local that wind speed and surface source intensity can be taken as nearly constant. With these findings, noise intensity can be well approximated as the product of a local universal ambient noise source factor and a waveguide propagation factor even for the range-dependent wind speeds of a hurricane.

At low frequencies, below roughly 100 Hz, we show that attenuation by wind-induced bubbles in the upper-ocean boundary layer should be insignificant even in hurricane conditions. *Temporal variations* in underwater noise intensity should then be primarily caused by the universal ambient noise source factor which is expected to depend on local wind speed and will vary as a hurricane advects over a fixed receiver. By extrapolating known relationships[14] between wind speed and noise level in this frequency range, the ambient noise level should increase monotonically with wind speed, and it should be possible to directly estimate local wind speed from measured noise level.

At higher frequencies temporal variations in underwater noise intensity may also be caused by attenuation due to scattering from bubbles in the upper-ocean boundary layer. This attenuation increases with wind speed and acoustic frequency. Farmer and Lemon[16] experimentally show that this leads to a frequency-dependent peak in noise level versus wind speed at frequencies above 8 kHz and wind speeds above 15 m/s. We analytically show that such a peak may also exist for frequencies above 100 Hz in typical hurricane wind speeds. Since the shape of the ambient noise versus wind speed curve and the location of its peak vary strongly with frequency, we show that wind speed may still be unambiguously estimated from broadband ambient noise measure-

ments in hurricane conditions above 100 Hz once the corresponding universal source dependence is empirically determined.

The accuracy of underwater acoustic wind speed estimates depends on the signal-to-noise ratio (SNR) of the underwater ambient noise intensity measurements upon which they are based. Piggott[14] and Perrone[17] have consistently measured wind noise with a standard deviation of less than 1 dB, as expected from theory where the variance of the intensity measurement can be reduced by stationary averaging.[8,18,19] For the measured power-law relationships that range from quartic to square,[11,14] a 1-dB standard deviation in sound pressure level corresponds to a 6% to 12% respective error in estimated wind speed. If realizable in hurricane conditions, this may provide a useful alternative to current satellite-based techniques.

Ocean acoustics then has serious potential for providing accurate and inexpensive hurricane classification estimates. Since a single hydrophone effectively measures only the local surface noise, it will effectively cut a swath through the hurricane, yielding local wind speed estimates as the storm passes over. At low frequencies, current evidence suggests a simple power-law relationship between noise intensity and wind speed. At higher frequencies, a frequency-dependent roll-off is expected in the relationship due to attenuation by bubbles. Wind speed can still be uniquely estimated, however, by making broadband measurements at higher frequency.

While current satellite technology has made it possible to effectively detect and track hurricanes, it is still difficult to accurately measure the wind speeds and classify the destructive power of a hurricane from satellite measurements. The standard method for hurricane classification by satellite, the Dvorak method,[20–23] often yields errors in wind speed estimates as high as 40%.[24–28] For example, of the eight North Atlantic hurricanes of 2000, three of them[24–26] experienced Dvorak errors over 40% and three more[29–31] experienced Dvorak errors over 20% when compared to the best estimate of wind speed from aircraft measurements. Several satellite microwave techniques show some promise for measuring hurricane wind speed[32] but, because of resolution and accuracy issues, the Dvorak method is still the standard for satellite hurricane classification.[23] In the North Atlantic the limitations of satellite technology are overcome by use of reconnaissance aircraft. These fly through the center of a hurricane to make the accurate measurements of wind speed necessary for classification. Unfortunately the expense of these aircraft prevents their routine use outside the United States.[33] For example, the cost to purchase a WC-130 aircraft is roughly $78 million,[34] adjusted for inflation to year 2003 dollars, and the deployment cost is $155 000 per flight.[35]

Classification of a hurricane's total destructive power, which is proportional to the cube of the hurricane's maximum wind speed,[36] is critical for hurricane planning. For example, inaccurate classification can lead to poor forecasting and unnecessary evacuations,[37] which are expensive, or missed evacuations, which can result in loss of life. These fatalities and costs can be reduced if the public is given timely and accurate advanced warning, but this depends on the ability to accurately classify hurricanes while they are still far from land. To give some background, in 1992 Hurricane Andrew became the most costly natural disaster in United States history causing an estimated 25 billion dollars in damage[33,38] and in 1900 an unnamed hurricane became the most deadly disaster in United States history killing over 6000 people.[39] Overseas the worst hurricane in history killed over 300 000 people in Bangladesh in 1970.[33]

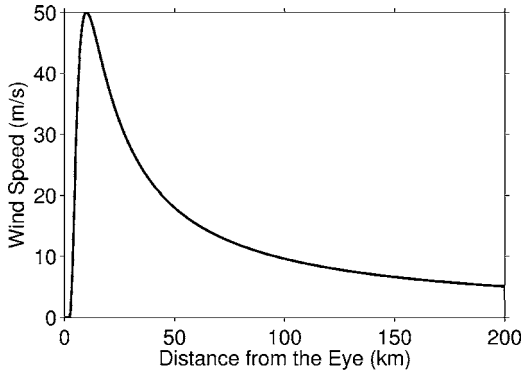

FIG. 1. Hurricane wind speed as a function of distance from the hurricane center based on Holland's model[36] with parameters $A=72.44$, $B=1.86$, $p_c=96\,300$ Pa, $p_n=100\,500$ Pa, and $\rho_{\mathrm{AIR}}=1.15$ kg/m^3. The zero wind speed region at the center of the hurricane (0 km) is called the eye and the high wind speed region (10 km) is the eye wall. The total destructive power of the hurricane is proportional to the cube of the maximum wind speed, which occurs in the eye wall.[40]

In this paper we review models for the spatial wind speed dependence of a hurricane that will be used to model ambient noise, past experiments that measured the relationship between underwater noise intensity and wind speed, and models for range-dependent noise in the ocean. We then develop a model for wind generated noise from a hurricane for both single sensors and arrays. We use this model to demonstrate the potential usefulness of classifying hurricanes with underwater acoustic sensors.

II. HURRICANE STRUCTURE AND CLASSIFICATION

Hurricanes are severe storms characterized by surface winds from 33 to over 80 m/s (Ref. 33) that circulate around a central low pressure zone called the eye. Holland[36] gives an analytic model for the surface wind speed profile as a function of range from the eye since hurricanes are typically cylindrically symmetric,

$$V=\sqrt{AB(p_n-p_c)\frac{\exp\{-A/r^B\}}{\rho_a r^B}} \tag{1}$$

where V is wind speed at a height of 10 m above the sea surface, p_c and p_n are the atmospheric pressure in the eye and outside the hurricane, respectively, ρ_a is the density of the air, and A and B are empirical values. Using this model, the surface wind speed profile for a moderate hurricane is given in Fig. 1, where wind speed in the eye is zero and rapidly increases to a maximum of 50 m/s at what is known as the eye wall. Outside of the eye wall, which is on the order of 10 km thick, wind speed slowly decreases to the edge of the hurricane which is typically hundreds of kilometers from the eye. Most of a hurri-

cane's destructive power then comes from the high winds in the eye wall since this power is roughly proportional to the cube of the maximum wind speed.[40]

The standard approach for classifying a hurricane's destructive power, the Dvorak method,[20–22] is effectively a pattern-recognition technique where satellite images, in the visible and infrared spectrum, are used to classify the hurricane based on features like the size and the geometry of cloud patterns. As discussed in the Introduction, this method often yielded wind speed estimates with errors of over 40% in several recent hurricanes.[24–28] Despite these errors, the Dvorak method is still the primary technique for classifying the destructive power of a hurricane from satellite measurements.[23] A satellite-based pattern-recognition technique similar to the Dvorak method using SSM/I satellite microwave (85 GHz) instead of optical and infrared images has recently been developed but gives similar errors to the Dvorak method.[41]

Satellite classification of hurricanes with microwave sounding units (MSU)[42] is secondary to the primary Dvorak method[23] due to the limited spatial resolution of the unit. The 55-GHz microwave radiation given off by warm air in the hurricane's eye is used to estimate temperature and then infer the hurricane's power. Because of the small size of the satellite array its spatial resolution is about 48 km,[43] which is often larger than the diameter of the eye, resulting in a blurred image of the hurricane and potential errors in estimates of destructive power.[42,43]

Other satellite techniques for estimating hurricane wind speed and destructive power are under development. For an overview see the article by Katsaros *et al.*[32] These techniques, however, are not yet used operationally for hurricane classification and disaster planning.[44]

To overcome the limitations of satellite techniques, specially equipped aircraft, like the Air Force's WC-130s and NOAA's WP-3s, are flown through the center of a hurricane.[44] Using on-board sensors and expendable dropsondes, accurate wind speed estimates with errors less than 5 m/s can be obtained.[44] Unfortunately these aircraft are expensive to purchase and operate and are currently only used by the United States.[33]

III. WIND-GENERATED SURFACE NOISE

Here we develop a model for the surface-generated noise intensity and mutual intensity from a hurricane received by a hydrophone or hydrophone array submerged in an ocean waveguide. The geometry of the problem is shown in Fig. 2. The hurricane is centered at the origin and is surrounded by ambient winds, all of which cause local sea-surface agitation. This agitation leads to sound sources with amplitude dependent on the local wind speed, modeled as a sheet of monopoles on a source plane at a depth z_0 within a quarter wavelength of the free surface following ocean acoustic noise modeling convention.[5–7] Intensity and mutual intensity are determined by directly integrating the surface source contributions using the waveguide Green function.

Several previous authors have addressed similar surface noise problems; however, their derivations are intertwined

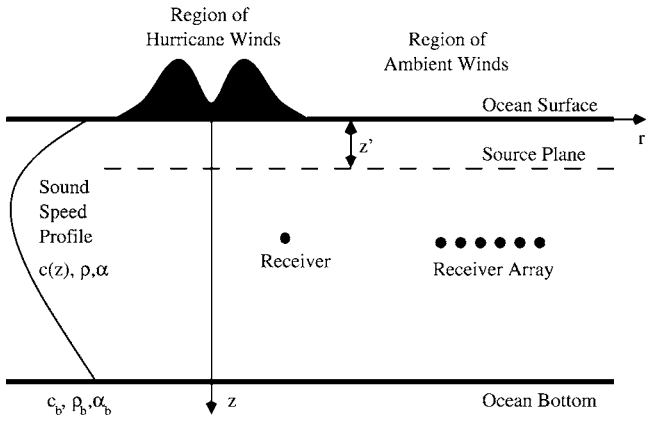

FIG. 2. Cross section of the stratified ocean waveguide showing the geometry of the surface noise problem (not to scale). On the surface is the area covered by the hurricane and surrounding area covered by 5 m/s ambient winds. The surface noise sources are modeled as a plane of monopoles a small depth z_0 below the surface and the sound field is measured by a single point receiver or reciever array.

with approximations or parametrizations that are not suitable for modeling hurricane noise. Kuperman and Ingenito[5] developed a widely used surface noise model; however, embedded in their derivation is the assumption that the source field is range independent. This is not true for hurricane-generated noise where the wind speed and source level change drastically with position.

Using an adiabatic normal mode formulation Perkins *et al.*[7] extended the model of Kuperman and Ingenito to range-dependent source fields and mildly range-dependent waveguides. They did this by dividing the surface area into smaller subareas over which the source field could be considered constant. They used far-field approximations for each subarea. These were coupled with the further approximation that the cross-spectral density for each subarea could be expressed as a single sum over modes. This approximation is only valid when the inverse of the difference between the horizontal wavenumber of the modes is much less than the dimension of the subarea.[45,46] For the highly range-dependent winds of a hurricane in an otherwise range-independent waveguide, this approach proves to be less accurate, more cumbersome, and less efficient to implement than direct integration.[47] Carey *et al.*[6] have developed a computational approach based on the parabolic equation approximation for calculating range-dependent surface noise. We find that steep angle contributions dominate the intensity measured by a single sensor and so require direct integration of local noise sources with a full-field model for the Green function rather than an elevation-angle-restricted parabolic approximation.

It is useful to briefly derive the direct integration approach used here since it has not explicitly appeared in the previous literature even though many essential elements are implicit in the work of Perkins *et al.*[7] For uncorrelated sources the cross-spectral density of the noise field can be written as

$$C(\mathbf{r_1},\mathbf{r_2},f)=\int_{\infty} d^2\boldsymbol{\rho_0}\frac{S_{qq}(V(\boldsymbol{\rho_0}),f)}{\Delta A}g(\mathbf{r_1}|\mathbf{r_0},f)g^*(\mathbf{r_2}|\mathbf{r_0},f) \tag{2}$$

as shown in Appendix A where $S_{qq}(V(\boldsymbol{\rho_0}),f)$ is the source power-spectral density, which is a function of wind speed V and frequency f, ΔA is a small area increment of integration at least the size of the horizontal coherence area of the source distribution, and $g(\mathbf{r_j}|\mathbf{r_0},f)$ is the waveguide Green function. Throughout this paper a cylindrical coordinate system in used where $\mathbf{r}=(\boldsymbol{\rho},z)=(\rho,\theta,z)$, $\boldsymbol{\rho}$ is the horizontal location vector, ρ is distance from the origin, θ is azimuth angle, and z is depth measured with positive downward from the surface. The locations $\mathbf{r_1}$ and $\mathbf{r_2}$ are receivers and $\mathbf{r_0}$ is the source. Green functions are calculated by a combination of wavenumber integration at short ranges and the normal mode approximation at long ranges. The integration over surface source area is computed numerically. This expression is valid for range-dependent source fields and environments.

The source depth z_0 is taken to be a quarter wavelength for all simulations in the present paper. This follows noise modeling convention[5–7] since source depths of a quarter wavelength or less lead to a downward-directed dipole source radiation pattern. Hamson has shown that on average wind-generated noise in the ocean radiates with a downward directed pattern that closely fits a dipole for wind speeds between 5 and 20 m/s and frequencies from 400 Hz to 3.2 kHz.[48] This is true even for average source depths greater than a quarter wavelength and sea-surface roughness much larger than the wavelength[48,49] as in a hurricane where wave heights may exceed 10 m. This is understandable since surface noise is believed to arise from many monopole sources, in particular bubbles, randomly distributed near the sea surface. All of these, by the method of images, have main downward directed lobes and varying side-lobes which tend to cancel.

As discussed in the Introduction, the source power-spectral density has been shown to follow

$$S_{qq}(V,f)=s_0(f)V^{n(f)} \tag{3}$$

for certain frequency and wind speed ranges. While experiments[14] at wind speeds below 20 m/s give $n=3.1\pm0.3$, values in the broader $n=1$ to $n=4$ range will be used here for illustrative purposes. If it is later found that wind speed and noise intensity are related by some other function, the power-law relationships considered here will provide a basis for piecewise construction of this more complicated dependence.

Farmer has shown experimentally that clouds of bubbles near the ocean surface may, through scattering and absorption, lower ambient noise levels at frequencies above 8 kHz and wind speeds above 15 m/s.[16] While such attenuation has never been observed at lower frequencies, we will consider its possibility in the high winds of a hurricane.

Attenuation, in dB/m, can be written as $\alpha=10\log(e)\sigma n_v$, where σ is the extinction cross section of an individual bubble and n_v is the number of bubbles per unit volume.[15] Using this expression, Weston[15] provides a model for attenuation by sea surface bubble clouds, based on the extinction cross section and spatial distribution of wind-generated bubbles as a function of wind speed and frequency. This attenuation can then be included in the Green function in Eq. (2) to determine its effect on the underwater noise field. This is done by calculating the Green function for a waveguide with an effective attenuation in dB/m of

$$\alpha(V,f)=\begin{cases}9.35\times10^{-7}\sqrt{f}V^3, & f<1.5\text{ kHz},\\ 2.44\times10^{-8}fV^3, & f>1.5\text{ kHz},\end{cases} \tag{4}$$

in a layer at the sea surface as given by Weston.[15]

IV. SINGLE HYDROPHONE ANALYSIS

Here it is shown that the noise intensity measured by a single sensor in a hurricane is dominated by local sea-surface sources rather than sound propagating from longer ranges. Underwater acoustic intensity can then be used to estimate the wind speed within a local resolution area since wind speed in a hurricane is also found to be effectively constant over this scale.

Beginning with the cross-spectral density of the noise field in a hurricane, Eq. (2), the spectral intensity of the sound field received at $\mathbf{r}$ can written as

$$I(\mathbf{r},f)=\frac{C(\mathbf{r},\mathbf{r},f)}{\rho_w c}=\int_{-\infty}^{\infty} d^2\boldsymbol{\rho_0}\frac{S_{qq}(V(\boldsymbol{\rho_0}),f)}{\rho_w c\Delta A}|g(\mathbf{r}|\mathbf{r_0},f,V(\boldsymbol{\rho_0}))|^2, \tag{5}$$

where the total instantaneous intensity is given by

$$\mathcal{I}(\mathbf{r})=\int_0^{\infty} I(\mathbf{r},f)df. \tag{6}$$

The Green function $g(\mathbf{r}|\mathbf{r_0},f,V(\boldsymbol{\rho_0}))$ depends on local wind speed $V(\boldsymbol{\rho_0})$ because it includes attenuation due to wind-generated sea-surface bubbles. We show that this wind speed dependence is negligible at frequencies less than 100 Hz for typical hurricane wind speeds, but needs to be accounted for at higher frequencies. Surface wind speed V is given by the Holland model of Fig. 1 for a hurricane, while the surrounding ambient wind speed is taken to be 5 m/s.

Two hurricane-prone ocean environments surrounded by densely populated coastal communities, the North Atlantic and the Bay of Bengal, are considered. Their sound speed profiles are shown in Fig. 3. The difference in water depth between these two environments leads to fundamental differences in propagation. Typical near-surface sound sources will lead to refractive propagation with excess depth in the North Atlantic but not in the Bay of Bengal. In the former, sound may propagate efficiently to long ranges via the deep-sound channel, while in the latter, it will multiply reflect from the lossy bottom leading to far greater transmission loss. Although hurricanes decrease the temperature of the local sea surface by roughly 1 °C near the eye wall to roughly 35-m depth, the corresponding small change in sound speed[50] of roughly 4 m/s is also local and so has a negligible effect on the curvature of both local and long-range sound paths.

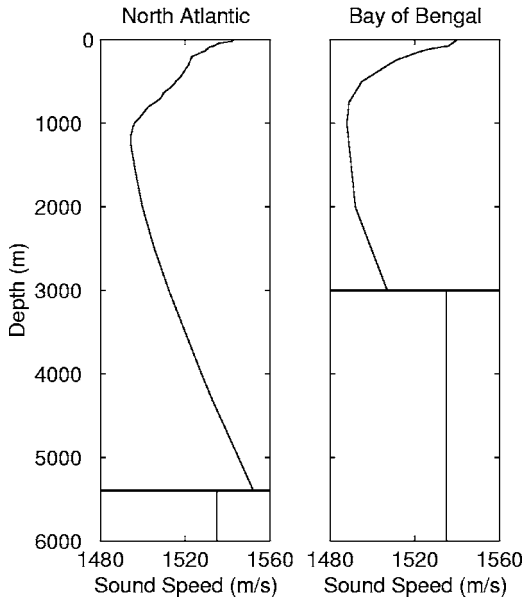

FIG. 3. Sound speed profiles $c(z)$ for the North Atlantic[65] and the Bay of Bengal.[66,67] The bottom has a density of 1.38 g/cm and an attenuation of 0.3 dB/λ corresponding to the deep silty sediment layers of the Bay of Bengal[68,69] and the North Atlantic Abyssal plain.[70,71] The water has a density of 1 g/cm and an attenuation of 6×10^{-5} dB/λ.

The spectral intensity level, given by

$$L_I = 10\log\left(\frac{I(\mathbf{r},f)}{I_{\mathrm{ref}}(f)}\right) \tag{7}$$

in dB *re* $I_{\mathrm{ref}}(f)$, of hurricane-generated noise is computed by the direct integration of Eq. (5) as a function of receiver range ρ and depth z from an origin at the center of the hurricane on the sea-surface. For convenience in the present paper the reference level $I_{\mathrm{ref}}(f)$ is taken to be the spectral intensity at a reference depth $z_{\mathrm{ref}}=200$ m for a reference 10-m altitude wind speed of $V_{\mathrm{ref}}=5$ m/s over the entire ocean

$$I_{\mathrm{ref}}(f) \equiv I(\mathbf{r}_{\mathrm{ref}},f) = \int_{-\infty}^{\infty} d^2\boldsymbol{\rho_0}\frac{S_{qq}(V_{\mathrm{ref}},f)}{\rho_w c\Delta A}|g(\mathbf{r}_{\mathrm{ref}}|\mathbf{r_0},f,V_{\mathrm{ref}})|^2, \tag{8}$$

where $\mathbf{r}_{\mathrm{ref}}=(\boldsymbol{\rho},z_{\mathrm{ref}})$. Noise intensity has been measured for 5 m/s wind speed in many ocean environments and at similar depths.[14,17,51,52] In an experimental scenario other reference values could be chosen.

Spectral intensity level is shown in Fig. 4 for frequencies of 50, 400, and 3200 Hz, spaced three octaves apart, using Eqs. (3)–(8) and assuming $n=3$. The choice of $n=3$ is within measured power-laws[14] and has been chosen out of convenience since it is linearly related to the power of the wind.[53] The wind speed profile of the hurricane and surroundings based on the Holland model at an altitude of 10 m from the sea surface is also plotted with the spectral intensity level at a depth of 200 m. The most apparent feature in Figs. 4(a) and 4(c) is the effectively linear relationship at low frequency, 50 Hz, between spectral intensity level L_I and the log of the wind speed. This is roughly independent of depth as can be seen in Figs. 4(b) and 4(d). At higher frequencies,

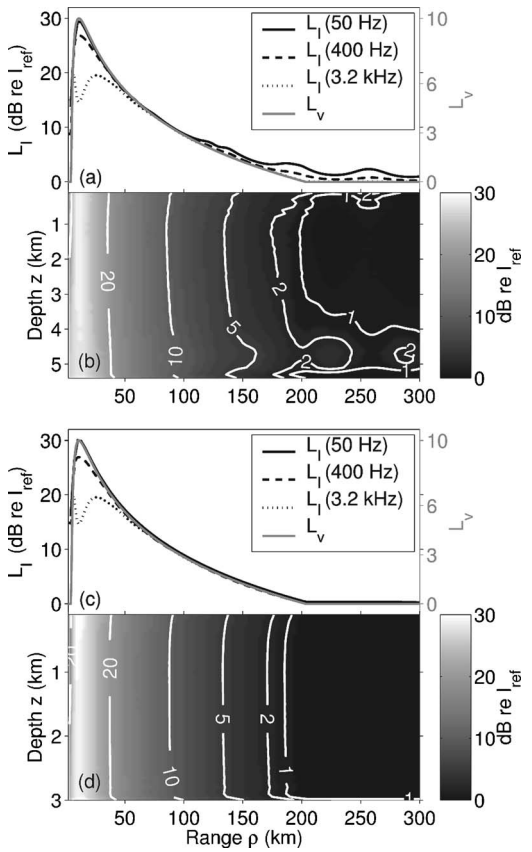

FIG. 4. Noise spectral level (dB *re* I_{ref}) in the North Atlantic [(a) and (b)] and the Bay of Bengal [(c) and (d)] for $n=3$. (a) and (c) show the level as a function of range at a depth of 200 m for 50, 400, and 3200 Hz frequencies. $L_V(\boldsymbol{\rho})=10\log(V(\boldsymbol{\rho})/V_{\mathrm{ref}})$ is plotted for comparison where $V_{\mathrm{ref}}=5$ m/s. $L_V=0$ is equivalent to $V=5$ m/s and $L_V=10$ is equivalent to $V=50$ m/s. (b) and (d) show the level as a function of range and depth at 50 Hz. In both waveguide environments the noise level closely follows the local wind speed. In the North Atlantic there is a convergence zone structure due to sound that propagates from the hurricane's eye wall. Note the convergence zone near the surface at a range of 257 km and the ray vertex depth of 4.7 km.

sea-surface bubbles significantly attenuate sound in the high-wind-speed, eye-wall region of the hurricane but the noise still follows local wind speed with a more complicated nonlinear dependence as will be shown in the next section. The small increase in level in the North Atlantic outside the hurricane at ranges of 193 and 257 km and at a depth of 4.7 km is caused by convergence zone propagation from the powerful sources in the eye wall. This convergence zone structure indicates an efficient mechanism exists for the long-range propagation of hurricane noise in this environment that will be considered in Sec. V.

A. Local noise dominates

The effectively linear relationship between the log of local wind speed and underwater acoustic spectral intensity shown in Fig. 4 suggests a possible simplifying approximation to our formulation. In particular the areal integral of Eq. (5) can be approximated by integrating only over local sources in the hurricane. These fall within a disc of area $A=\pi R^2$ centered at the horizontal location of the receiver $\boldsymbol{\rho}$

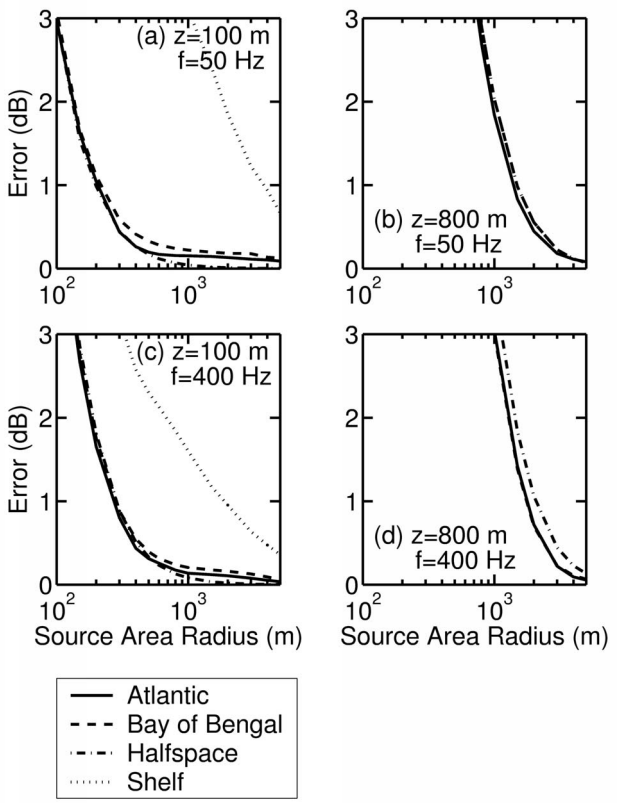

FIG. 5. Error induced by the local area approximation [Eq. (9)] as a function of local source area radius R_{local} for a single sensor under the maximum winds in the eye wall of a hurricane. Curves are shown for the North Atlantic and the Bay of Bengal environments used in this paper as well as for infinite half-space and shallow water continental shelf environments. Plots are given for sensor depths of 100 m [(a) and (c)] and 800 m [(b) and (d)] and for frequencies of 50 Hz [(a) and (b)] and 400 Hz [(c) and (d)]. While these plots are given for $n=3$ the difference for values $n=1$ to 4 is less than 0.1 dB. The North Atlantic, Bay of Bengal, and infinite half-space environments are very similar. In these deep-water environments, for the shallow 100-m sensor depth, we see that for R_{local} greater than 300 m the approximation error is negligible. For the deeper 800-m sensor depth, the R_{local} for which the error is negligible is roughly 2 km. In shallow water the error in the local area approximation is higher leading to a larger R_{local}. This is likely due to the strong reflection of sound off bottom. In deep water environments bottom reflections have little effect and most of the sound measured by a receiver propagates via direct path from the surface source.

which provides the dominant contribution in the exact integral [Eq. (5)]. The spectral intensity can then be approximated as

$$I(\mathbf{r},f) \approx \int_A d^2\boldsymbol{\rho}_\mathbf{0}' \frac{S_{qq}(V(\boldsymbol{\rho}_\mathbf{0}'),f)}{\rho_w c \Delta A} |g(\mathbf{r}|\mathbf{r}_\mathbf{0}',f,V(\boldsymbol{\rho}_\mathbf{0}'))|^2 \tag{9}$$

where $\boldsymbol{\rho}_\mathbf{0}'=\boldsymbol{\rho}_\mathbf{0}-\boldsymbol{\rho}$. Such a simplification can potentially lead to errors if R is too small.

To quantify the potential error of this local approximation, the approximate equation (9) is evaluated for a receiver under the eye wall of the hurricane where wind speed varies most drastically. When compared to the exact result of Eq. (5), we take the error induced by the local approximation to be negligible, less than or equal to 1 dB, for R greater than a minimum length R_{local}. The error as a function of R is given in Fig. 5 where, for deep-water environments, $R_{\text{local}}=300$ to 2000 m depending on sensor depth.

It is noteworthy that the deep-ocean North Atlantic and Bay of Bengal error curves closely match those of the infinite half-space. This shows that bottom reflections and variations in sound speed profile do not have a significant effect on R_{local} in deep water. For a bottom-mounted sensor in a typical shallow water environment $R_{\text{local}}=2$ to 3 km in the 50 to 400 Hz range. Our computations also show that R_{local} does not change significantly for the expected source power-spectral densities and attenuations considered in this paper.

The wind speeds in a hurricane do not change significantly over R_{local} and can be approximated as constant in Eq. (9). This leads to less than 0.2 dB additional error in the spectral intensity level, which can then be approximated as

$$\begin{aligned} I(\mathbf{r},f) &\approx \frac{S_{qq}(V(\boldsymbol{\rho}),f)}{\rho_w c \Delta A} \int_0^{2\pi} \int_0^{R_{\text{local}}} \rho_0' d\rho_0' d\theta_0' |g(\mathbf{r}|\mathbf{r}_\mathbf{0}',f,V(\boldsymbol{\rho}))|^2 \\ &\equiv S_{qq}(V(\boldsymbol{\rho}),f) W(\mathbf{r},f,V(\boldsymbol{\rho})) \end{aligned} \tag{10}$$

where only the local wind speed $V(\boldsymbol{\rho})$ directly above the receiver has a significant effect on both the source factor $S_{qq}(V(\boldsymbol{\rho}),f)$ and the waveguide propagation factor $W(\mathbf{r},f,V(\boldsymbol{\rho}))$. The source factor is universal in that it does not depend on propagation parameters and should be the same for any waveguide environment so long as the ocean depth greatly exceeds the ocean-atmosphere boundary layer. While the propagation factor does depend on the environment, ocean waveguides typically change gradually with horizontal position. The wind-speed-independent functionality of $W(\mathbf{r},f,V(\boldsymbol{\rho}))$ should then be effectively constant over R_{local} and over the horizontal extent of a hurricane, on the order of 100 km. Both factors may be characterized numerically or empirically to develop a set of curves to estimate wind speed from acoustic intensity. In the next section we find that it is possible to simplify these factors and develop an approximate analytic equation for wind speed estimation.

The approximate Eq. (10) for *range-dependent* sources and potentially *range-dependent* waveguides is similar to Kuperman and Ingenito's[5] exact Eq. (30) for *range-independent* sources and waveguides in that spectral intensity is the product of a "universal ambient noise" source factor, following Ingenito and Wolf[9] and here defined as $S_{qq}(V(\boldsymbol{\rho}),f)$, and a waveguide propagation factor $W(\mathbf{r},f,V(\boldsymbol{\rho}))$. The implicit assumption of formulations of this kind is that variations in source depth can be accounted for as equivalent variations in $S_{qq}(V(\boldsymbol{\rho}),f)$. This is consistent with the measured dipole behavior of ambient noise in the ocean.[48]

Taking the log of Eq. (10) leads to a useful approximate equation for spectral intensity level,

$$L_I(\mathbf{r},f) \approx L_S(V(\boldsymbol{\rho}),f) + L_W(\mathbf{r},f,V(\boldsymbol{\rho})) \tag{11}$$

in dB *re* $I_{\text{ref}}(f)$ where

$$L_S(V(\boldsymbol{\rho}),f) = 10\log\left(\frac{S_{qq}(V(\boldsymbol{\rho}),f)}{S_{qq}(V_{\text{ref}},f)}\right), \tag{12}$$

$$L_W(\mathbf{r},f,V(\boldsymbol{\rho})) = 10\log\left(\frac{W(\mathbf{r},f,V(\boldsymbol{\rho}))}{W_{\text{ref}}(f)}\right), \tag{13}$$

and

$$I_{\text{ref}}(f) = S_{qq}(V_{\text{ref}},f)W(\mathbf{r}_{\text{ref}},f,V_{\text{ref}}) = S_{qq}(V_{\text{ref}},f)W_{\text{ref}}(f). \tag{14}$$

Here $L_S(V(\boldsymbol{\rho}),f)$ is a universal ambient noise source term that is independent of waveguide propagation parameters, while $L_W(\mathbf{r},f,V(\boldsymbol{\rho}))$ is a waveguide propagation term. The functional dependencies of the first term can be determined empirically in any waveguide where the ocean depth greatly exceeds the ocean-atmosphere boundary layer, while the functional dependencies of the second term should be locally determined.

If $S_{qq}(V(\boldsymbol{\rho}),f)$ follows a power-law, such as Eq. (3), then universal ambient noise source level is linearly related by

$$L_S(V(\boldsymbol{\rho}),f) = 10n(f)\log\left(\frac{V(\boldsymbol{\rho})}{V_{\text{ref}}}\right) \tag{15}$$

to the log of wind speed. The slope of this linear relationship $10n(f)$ has been previously measured in the 13 Hz to 14.5 kHz frequency range and 1 to 20 m/s wind speed range.[10,11,14,51,52]

To estimate wind speed from ambient noise measurements using Eq. (11), the dependence of $L_W(\mathbf{r},f,V(\boldsymbol{\rho}))$ on wind-dependent attenuation by sea-surface bubbles needs to be established. This may be done empirically, numerically, or analytically as in the next section.

B. Separating the effect of attenuation by bubbles from local waveguide propagation

Analytic expressions are derived to show how attenuation can be separated from other waveguide propagation effects so that $L_W(\mathbf{r},f,V(\boldsymbol{\rho}))$ can be split into a universal wind-speed-dependent attenuation term and a local waveguide calibration term that is wind-speed independent. These analytic expressions also demonstrate the uniqueness of a wind speed estimate based on broadband underwater noise measurements. They also enable analytic expressions for estimation error to be obtained in some important cases.

Underwater spectral intensity level is calculated over a range of wind speeds and frequencies relevant to hurricane classification as illustrated in Fig. 6 using the full areal integration of Eq. (5). The spectral intensity level exhibits a maxima that depends on wind speed and frequency. For wind speeds and frequencies below this maxima, attenuation by bubbles is negligible so that $L_W(\mathbf{r},f,V(\boldsymbol{\rho}))$ is only a function of the local waveguide environment and spectral intensity level $L_I(\mathbf{r},f)$ should depend on the log of wind speed only through Eq. (15) given the power-law $n=3$ assumption of the simulation. For higher wind speeds and frequencies, attenuation by bubbles is significant and eventually leads to a roll-off in the spectral intensity so that $L_W(\mathbf{r},f,V(\boldsymbol{\rho}))$ is a separable function of both wind-speed-dependent and wind-speed-independent terms.

While the dependence of spectral intensity on wind speed and frequency including attenuation by bubbles can be

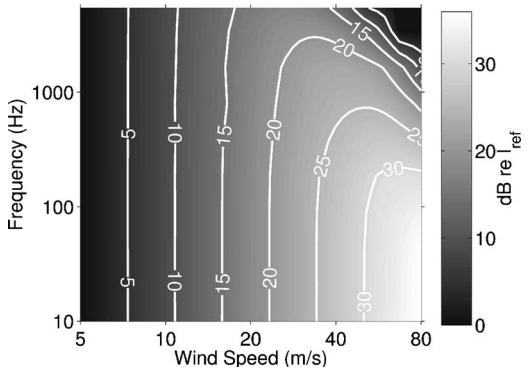

FIG. 6. Simulated noise spectral level (dB *re* I_{ref}) in the North Atlantic for range-independent winds as a function of wind speed and frequency including attenuation by sea-surface bubbles assuming $n=3$ from Eq. (5). Below 100 Hz the power-law relationship between noise intensity and wind speed is unaffected by bubble attenuation even up to the 80 m/s wind speeds of a hurricane. As frequency increases, attenuation affects the noise level at progressively lower wind speeds. For a given frequency the noise level increases linearly with wind speed, peaks, and then decays exponentially.

calculated exactly using the full areal integration of Eq. (5) or the local integral approximations of Eqs. (9) and (10), a useful first-order approximation leads to the analytic result

$$W(\mathbf{r},f,V(\boldsymbol{\rho})) = W_0(\mathbf{r},f)\frac{4\pi^2|A(V(\boldsymbol{\rho}),f,k_r=0)|^2}{z_0^2}, \tag{16}$$

where

$$W_0(\mathbf{r},f) = W(\mathbf{r},f,0) \tag{17}$$

and

$$A(V(\boldsymbol{\rho}),f,k_r=0) = \frac{\sin(kz_0)}{2i\pi[\alpha/(20\log(e))]\cos(kL) + [2\pi\omega/c(z_0)]e^{-ikL}} \tag{18}$$

is the downward plane-wave amplitude for a source in an attenuating sea-surface bubble layer following the Pekeris solution.[54] The complex wavenumber

$$k = \frac{\omega}{c(z_0)} + i\frac{\alpha(V(\boldsymbol{\rho}),f)}{20\log(e)}$$

is used in Eq. (18) where $\alpha(V(\boldsymbol{\rho}),f)$ is given in Eq. (4).

The spectral intensity level of Eq. (11) can then be approximated as

$$L_I(\mathbf{r},f) \approx L_S(V(\boldsymbol{\rho}),f) + L_A(V(\boldsymbol{\rho}),f) + L_{W_0}(\mathbf{r},f) \tag{19}$$

where

$$L_A(V(\boldsymbol{\rho}),f) = 20\log\left(\frac{2\pi|A(V(\boldsymbol{\rho}),f,k_r=0)|}{z_0}\right) \tag{20}$$

and

$$L_{W_0}(\mathbf{r},f) = 10\log\left(\frac{W_0(\mathbf{r},f)}{W_{\text{ref}}(f)}\right) \tag{21}$$

The approximation of Eq. (19) is in agreement with the full areal integration of Eq. (5) to within 1 dB for frequencies below 500 Hz even at hurricane wind speeds as shown in Fig. 7.

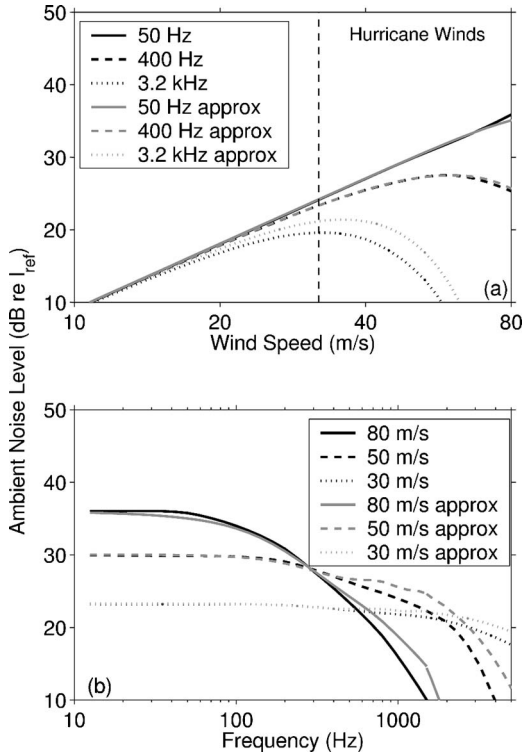

FIG. 7. (a) Noise spectral level (dB *re* I_{ref}) as a function of wind speed at several frequencies, assuming $n=3$. The black curves show the attenuation, caused by bubbles, at 50 Hz, 400 Hz, and 4 kHz. The range of wind speeds typical of a hurricane is also shown. (b) Noise spectral level curves as a function of frequency for typical hurricane wind speeds of 30, 50, and 80 m/s. The black curves show the full areal integration from Eq. (5) and the gray curves show the first-order approximation of the field given by Eq. (19) with Eqs. (15), (20), and (21).

By splitting the local waveguide and bubble attenuation effects of $L_W(\mathbf{r},f,V(\boldsymbol{\rho}))$ into two terms, $L_A(V(\boldsymbol{\rho}),f)$ and $L_{W_0}(\mathbf{r},f)$, wind speed can now be estimated from ambient noise using Eq. (19), where $L_A(V(\boldsymbol{\rho}),f)$ is a universal attenuation term that depends on local wind speed but like $L_S(V(\boldsymbol{\rho}),f)$ is also independent of waveguide parameters. The last term of Eq. (19), $L_{W_0}(\mathbf{r},f)$, is a local waveguide calibration that is independent of wind speed.

At frequencies below 100 Hz where attenuation α due to bubbles is negligible at hurricane wind speeds, $L_A(V(\boldsymbol{\rho}),f)$ goes to zero, as expected from Fig. 6. In this important case, if $S_{qq}(V(\boldsymbol{\rho}),f)$ follows a power law, Eq. (19) reduces to a linear equation in the log of wind speed,

$$L_I(\mathbf{r},f) \approx 10n(f)\log\left(\frac{V(\boldsymbol{\rho})}{V_{\text{ref}}}\right) + L_{W_0}(\mathbf{r},f), \tag{22}$$

where $10n(f)$ is a universal empirically determined slope and $L_{W_0}(\mathbf{r},f)$ is a local calibration intercept. The log of wind speed can be then found from measurements of ambient noise level by standard linear least squares estimation, as has been done in Refs. 10 and 11 at low wind speed.

As frequency increases, bubble-layer thickness exceeds a quarter wavelength and the $L_A(V(\boldsymbol{\rho}),f)$ term can be approximated as

$$L_A(V(\boldsymbol{\rho}),f) \approx -\alpha(V(\boldsymbol{\rho}),f)L. \tag{23}$$

If we use for illustrative purposes the $L=1.2$ m layer thickness given by Weston,[15] then Eqs. (20) and (23) agree to within 1 dB above 300 Hz and to within 2 dB between 100 and 300 Hz. While Weston notes that the assumption of a bubble layer of constant thickness may be poor at high wind speeds, any future improvements in our knowledge of the parameter L can be incorporated in Eqs. (18) and (23).

The locations of maxima in noise spectral level correspond to the ridge in Fig. 6. These can now be approximated analytically by substituting Eqs. (15), (21), and (23) into Eq. (19) and taking the derivative with respect to wind speed to obtain

$$V_{max} \approx \begin{cases} (1/(2.15\times10^{-7}L\sqrt{f}))^{1/3}, & 300 < f < 1.5 \text{ kHz}, \\ (1/(5.63\times10^{-9}Lf))^{1/3}, & f > 1.5 \text{ kHz}, \end{cases} \tag{24}$$

here assuming $n=3$ and $\alpha(V(\boldsymbol{\rho}),f)$ from Eq. (4).

C. Accuracy of underwater acoustic wind speed estimates

By standard stationary averaging, it should be possible to reduce the variance of an underwater acoustic wind speed estimate enough to be useful for meteorological purposes. Given the relationship $V=H(I)$ between the true wind speed V and true ambient noise intensity I, the maximum likelihood estimate (MLE) of the wind speed $\hat{V}$ given a measurement of ambient noise intensity $\hat{I}$ is $\hat{V}=H(\hat{I})$ by the invariance of the MLE.[55] The function H can be found either numerically from the exact integration, Eq. (5), or analytically from one of the approximations, Eqs. (11), (19), and (22). We define the percent root-mean-square error (RMSE) of the wind speed estimate $\hat{V}$ as

$$\nu_{\text{RMSE}} = 100\frac{\sqrt{\langle|\hat{V}-V|^2\rangle}}{\langle\hat{V}\rangle} \tag{25}$$

and the percent bias as

$$\nu_{\text{bias}} = 100\frac{|\langle\hat{V}\rangle - V|}{V} \tag{26}$$

given

$$\langle\hat{V}^m\rangle = \int_0^\infty H^m(\hat{I})p(\hat{I})d\hat{I}, \tag{27}$$

where $p(\hat{I})$ is the probability density function of the measured intensity $\hat{I}$. For the hurricane noise measurements considered here, where the contributions from a large number of independent sources are received simultaneously, the acoustic field is expected to be a circular complex Gaussian random variable. The time-averaged measured intensity $\hat{I}$ is then expected to follow a gamma distribution[8,19]

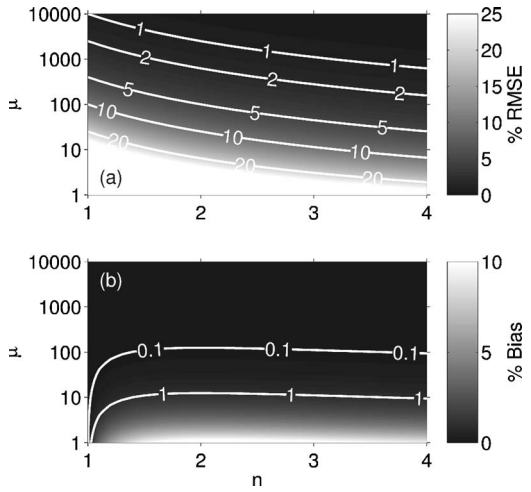

FIG. 8. The percent RMSE ν_{RMSE} (a) and percent bias ν_{bias} (b) of the wind speed estimate $\hat{V}$ where attenuation by sea-surface bubbles is insignificant, evaluated numerically from Eqs. (5) and (27). For time-bandwidth products $\mu > 5$ the estimate becomes unbiased and the RMSE attains the Cramer-Rao lower bound. Piggott[14] and Perrone[59] have measured wind noise level with standard deviations less than 1 dB which corresponds to $\mu > 19$. For $\mu = 19$ the percent RMSE in the wind speed estimate ranges from 6% to 25% depending on n which is a significant improvement over the primary satellite classification method.

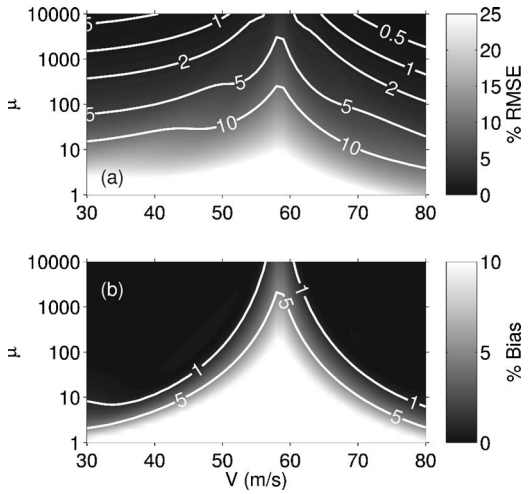

FIG. 9. The percent RMSE ν_{RMSE} (a) and percent bias ν_{bias} (b) of the wind speed estimate $\hat{V}$ including the effect of attenuation calculated numerically from Eqs. (5) and (27), assuming $n=3$, at $f=400$ Hz where $V_{\max}=58$ m/s. The error and bias increase for $V \approx V_{\max}$ but for $\mu > 5$ and for values of V where $\nu_{\mathrm{bias}} < 1\%$ the percent RMSE decreases and attains the Cramer-Rao lower bound. For spectral intensity measurements with $\mu = 19$ the percent RMSE in this example is between 9% and 20%.

$$p(\hat{I}) = \frac{(\mu/\bar{I})^{\mu}\hat{I}^{\mu-1}\exp\{-\mu(\hat{I}/\bar{I})\}}{\Gamma(\mu)}, \tag{28}$$

where μ is the time-bandwidth product and $\bar{I}$ is the mean of the noise measurement.

From the full areal integration of Eqs. (5) we can numerically find the percent RMSE and percent bias of the wind speed estimate $\hat{V}$. For frequencies below 100 Hz, where attenuation α is insignificant, we find that the percent RMSE and percent bias are functions of n and μ as shown in Fig. 8. At higher frequencies, where attenuation is significant, the percent RMSE and percent bias are also functions of frequency and wind speed. This is illustrated in Fig. 9 at a frequency of 400 Hz assuming $n=3$.

Following the standard practice of stationary averaging, the variance of noise measurements is reduced by inverse the number of stationary samples, $1/\mu$. In typical ocean acoustic applications, such as matched filtering, μ's in excess of 100 are common.[56–58] For example, Piggott[14] and Perrone[59] have obtained measurements of wind noise level with standard deviations less than 1 dB corresponding[8,18,19] to $\mu > 19$.

Given a spectral intensity measurement with $\mu > 19$, underwater acoustic wind speed estimates with errors similar to the 6% to 15% errors of hurricane-hunting aircraft[44] are possible. For example, at low frequencies where attenuation is insignificant, a measurement of noise spectral level with $\mu = 19$ would yield a corresponding percent RMSE in estimated wind speed of 6% to 25% for the range of published values for n as shown in Fig. 8. For the higher frequency 400 Hz example in Fig. 9, where attenuation is significant, a spectral intensity measurement with $\mu = 19$ will yield percent RMSEs from 9% to 20%. Even larger errors are common for remote satellite techniques, as high as 40% as noted in the Introduction. From this error analysis we find that underwater acoustic measurements may be worthwhile for estimating hurricane wind speed. Additional errors related to the practical application of the underwater acoustic technique will be discussed in Sec. IV D.

At low frequencies, less than 100 Hz, where attenuation α from bubbles becomes insignificant, the moments of $\hat{V}$ can also be evaluated analytically from the first-order approximation of Eq. (22) to illustrate the fundamental parameters affecting a wind speed estimate. The mean of the wind speed estimate can then be written as

$$\langle \hat{V} \rangle \approx \frac{\Gamma(\mu + 1/n)}{\Gamma(\mu)} \left(\frac{I(f)}{s_0 w_0 \mu} \right)^{1/n} = \frac{\Gamma(\mu + 1/n)}{\Gamma(\mu)\mu^{1/n}} V \tag{29}$$

and the standard deviation as

$$\sigma_{\hat{V}} \approx \left(\frac{I(f)}{s_0 w_0 \mu} \right)^{1/n} \sqrt{\frac{\Gamma(\mu + 2/n)}{\Gamma(\mu)} - \left(\frac{\Gamma(\mu + 1/n)}{\Gamma(\mu)} \right)^2}. \tag{30}$$

At these low frequencies the percent bias can then be approximated as

$$\nu_{\mathrm{bias}} \approx 100 \left| \frac{\Gamma(\mu + 1/n)}{\Gamma(\mu)\mu^{1/n}} - 1 \right| \tag{31}$$

and the percent RMSE as

$$\nu_{\mathrm{RMSE}} \approx 100 \sqrt{\frac{\Gamma(\mu + 2/n)\Gamma(\mu)}{\Gamma(\mu + 1/n)^2} - 2\frac{\Gamma(\mu)\mu^{1/n}}{\Gamma(\mu + 1/n)} + \frac{\Gamma(\mu)^2 \mu^{2/n}}{\Gamma(\mu + 1/n^2)}}. \tag{32}$$

These analytic expressions for the percent RMSE and percent bias match those calculated numerically from Eqs. (5) and (27) and shown in Fig. 8 to within 1%.

At low frequencies, where attenuation is insignificant, the Cramer-Rao lower bound can be derived from the first-

order approximation, Eq. (22), as shown in Appendix B. This provides a straightforward analytic method for calculating the percent RMSE as

$$\nu_{\mathrm{RMSE}} \approx 100\frac{\sqrt{Var_{\mathrm{asymptotic}}(\hat{V})}}{\langle \hat{V} \rangle} = 100\frac{1}{n\sqrt{\mu}}, \tag{33}$$

which matches the numerically computed value in Fig. 8 for $\mu > 5$. This is expected since the Cramer-Rao lower bound is the asymptotic variance for large μ. The Cramer-Rao lower bound can also be used to calculate the percent RMSE at frequencies above 300 Hz from the first-order approximation in Eqs. (19) with Eqs. (15), (21), and (23) yielding

$$\nu_{\mathrm{RMSE}} \approx 100\frac{\sqrt{Var_{\mathrm{asymptotic}}(\hat{V})}}{\langle \hat{V} \rangle} = 100\begin{cases} \dfrac{1}{\sqrt{\mu}(n - 6.46 \times 10^{-7} L\sqrt{f}V^3)}, & f < 1.5 \text{ kHz}, \\ \dfrac{1}{\sqrt{\mu}(n - 1.69 \times 10^{-8} LfV^3)}, & f > 1.5 \text{ kHz}, \end{cases} \tag{34}$$

which matches the numerical results in Fig. 9 when $\mu > 5$ and $\nu_{\mathrm{bias}} < 1\%$.

D. Practical issues

We have shown that a single underwater acoustic sensor provides significant potential as a measurement tool to accurately estimate local wind speed in a hurricane. There are practical issues, however, to consider when deploying such sensors to monitor a hurricane. While this is not a definitive discussion of all the issues that might be involved, we will attempt to illustrate how an underwater acoustic measurement system might be implemented. For example, how would one deploy these sensors, how many sensors would be needed to fully characterize a hurricane, and how much would it cost.

One possible scenario would be to deploy multiple sonobouys, similar to those used in weather classification experiments by Nystuen and Selsor,[60] from aircraft or ships in the path of an oncoming hurricane. As the hurricane passes over each sonobouy the sensor would cut a swath through the storm recording the wind speeds overhead. The swaths from multiple sonobouys could give a fairly complete measurement of the wind speeds in the hurricane. This is similar to the current measurements made by hurricane-hunting aircraft which fly through the storm cutting a swath and measuring wind speed. For both methods, sonobouys or hurricane-hunting aircraft, the sensors must pass through the eye wall of the hurricane where the winds are strongest. For aircraft this means actively piloting the plane through the storm, whereas with stationary sonobouys, one would deploy many sensors along a line that crosses the expected path of the hurricane to insure that at least one sonobouy cuts through the eye wall. For example, a line of 20 sonobouys spaced 5 km apart across the hurricane's path would span almost 100 km, assuring several measurements of the wind speed in the eye wall.

The advantage of deploying sonobouys in advance of a hurricane is that the ship or aircraft never has to enter the storm and would not need to be as expensive as the specialized hurricane-hunting aircraft used today. The cost of a typical hurricane-hunting aircraft such as the WC-130 is \$78 million (inflation adjusted to year 2003 dollars)[34] and the cost of a single flight[35] is roughly \$155,000. Between two and eight aircraft flights are made per day[44] for potentially landfalling hurricanes in the North Atlantic where the lifespan of a hurricane can be several weeks. Twenty sonobouys, at \$500 each,[61] could be deployed from inexpensive nonspecialized ships or aircraft in the path of an oncoming hurricane well before conditions are dangerous for roughly \$10,000.

An alternative scenario would be to deploy hundreds of permanent shore-cabled hydrophone systems, at \$10,000 to \$20,000 each depending on cable length, in strategic hurricane-prone areas for a few million dollars. As noted before, this is much less than the purchase price of a WC-130 hurricane-hunting aircraft.

Such underwater acoustic systems would likely be used in conjunction with *a priori* location estimates from satellites. Satellites would determine the path of the hurricane relative to the hydrophone and show whether the sensor passed through the high winds of the eye wall. The underwater acoustic measurement would then provide an estimate of the wind speeds for the portions of the hurricane that passed overhead. If a hydrophone does not pass through the powerful eye wall but rather through the weaker surrounding winds it would still provide a lower bound or threshold measurement of wind speed and it may be possible to extrapolate these lower wind speeds to determine the higher wind speeds of the eye wall.

V. HYDROPHONE ARRAY ANALYSIS

The analysis in the previous sections demonstrates how omnidirectional sensors may be used to accurately measure the local winds and classify the destructive power of a hurricane as it passes overhead. It may be possible to use arrays of hydrophones to beamform on the acoustic field from a hurricane at long range. For illustrative purposes we will consider horizontal linear arrays of the type that might be towed from an oceanographic or naval vessel; however, other array configurations, such as moored arrays, might also be useful. Arrays might also be useful for directionally filtering out other noise sources, such as ships and surf, in local measurements.

Using the expression for the cross-spectral density of the noise field of Eq. (2) we find the angular spectral density of the noise received by an N-element array, or beamformed output, to be

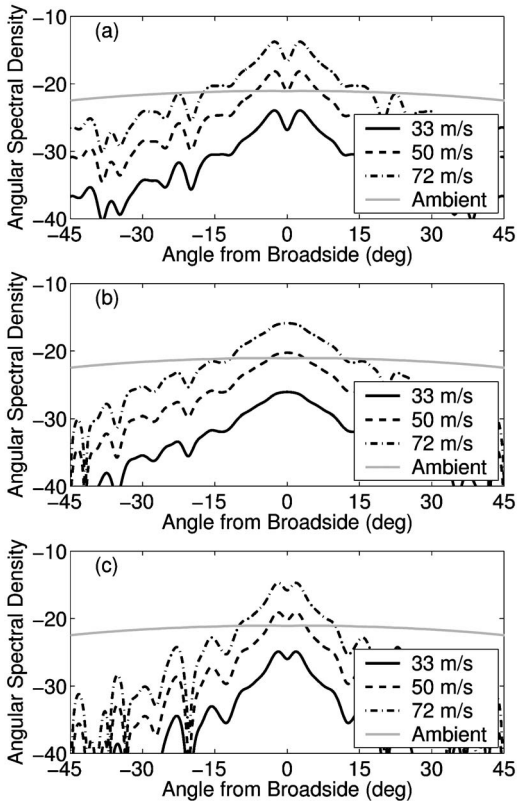

FIG. 10. Angular spectral density level $10\log(B(\Omega,f))\cdot(\mathrm{dB}\ re\ \rho_w c I_{\mathrm{ref}}/sr^2)$ at 100 Hz for a 64-element $\lambda/2$-spaced horizontal broadside array as a function of steering angle for hurricane-generated noise in the North Atlantic at ranges of 257 km (a), 289 km (b), and 385 km (c) from the eye of the hurricane, assuming $n=3$. Ranges of 257 and 385 km correspond to the fourth and sixth convergence zones from the center of the hurricane. The range of 289 km is exactly between the fourth and fifth convergence zones. Curves are shown for a powerful 72-m/s hurricane, a medium 50-m/s hurricane and a weak 33-m/s hurricane. The angular spectral density level from ambient noise is plotted for comparison. A steering angle of 0° corresponds to the array steered toward the calm eye of the hurricane and the powerful eye wall is located at ±3°. This array has an angular resolution of 1.8°, which at a range of 257 km corresponds to an 8-km spatial resolution.

$$B(\Omega,f)=\frac{1}{N^2}\sum_{m=1}^{N}\sum_{n=1}^{N}e^{-j\mathbf{k}\cdot\mathbf{r_m}}C(\mathbf{r_m},\mathbf{r_n},f)e^{j\mathbf{k}\cdot\mathbf{r_n}} \tag{35}$$

with units of $\mu\mathrm{Pa}^2/\mathrm{sr}^2$ Hz, where $\mathbf{k}=(2\pi f/c)\mathbf{i}_{\mathbf{\Omega}}$, $\mathbf{i}_{\mathbf{\Omega}}$ is a unit vector in the steering direction Ω, and $\mathbf{r_m}$ is the position of the mth hydrophone on the array.

We define the hurricane wind-generated noise source area to include sources within 200 km of the hurricane's center as shown in Fig. 1 and the ambient noise source area to include sources generated by the 5-m/s winds surrounding the hurricane. To show how an array might be able to measure the destructive power of a hurricane, the angular spectral density of the noise will be calculated for a hurricane as a function of maximum wind speed.

The angular spectral density of Eq. (35) in the direction of the hurricane increases with maximum wind speed, as shown in Fig. 10 for an array at 200-m depth at a range far from the hurricane eye. The difference in spectral density between the strong 72-m/s-wind-speed and weak 33-m/s-wind-speed hurricanes of Fig. 10 is roughly 10 dB given the assumption here that $n=3$. The difference in spectral density would be greater for larger n.

A practical horizontal array can resolve the important features of the hurricane such as the eye wall, which has dimensions of tens of kilometers, when placed in a convergence zone as in Figs. 10(a) and 10(c). This is not possible for an array just outside the convergence zone as shown in Fig. 10(b). In the former case, the length L of an array, oriented at broadside to the hurricane, would have to be

$$L>R\lambda/l \tag{36}$$

where R is the range from the array to the hurricane and l is the size of the eye-wall. Typical linear arrays[56] have lengths L on the order of $100\lambda/2$. In the example of Fig. 10, a broadside array with $L=32\lambda$, similar to the ONR FORA array,[62] images the hurricane with 10-km resolution at a range of 320 km. The width of the convergence zone must also be sufficiently small to resolve the eye wall in range. For the given environment and ranges considered, this condition is satisfied because the convergence zone width is roughly 5 km, which is less than the width of the eye wall.

A horizontal array oriented at end-fire to the hurricane has the advantage that it discriminates against local surface noise coming from near broadside in favor of sound that travels from long distances at shallow angles in the waveguide. This could potentially lead to longer hurricane detection ranges. Unfortunately, at end-fire, the length of the array must satisfy

$$L>2\lambda(R/l)^2 \tag{37}$$

to resolve the eye-wall. For example, an impractically long $L=2000\lambda$ end-fire array would be needed to achieve 10-km resolution at a range of 320 km.

The analysis presented here for the North Atlantic shows that it may be possible to image the features of a hurricane using linear broadside arrays of sufficient length. Waveguides that lack excess depth, such as the Bay of Bengal, do not exhibit the convergence zone structure seen in the North Atlantic. This probably makes it extremely difficult to even detect hurricanes using practical linear arrays at long ranges in these environments.

VI. CONCLUSIONS

We have shown that the wind-generated noise received by a single underwater acoustic sensor in a hurricane can be well approximated by sea-surface contributions so local that wind speed and surface source intensity can be taken as nearly constant. Two terms with empirically and analytically determined dependencies may be used to estimate wind speed from measured ambient noise spectral level: (1) a universal ambient noise source term and (2) a local waveguide calibration term. At low frequencies, current evidence suggests a simple power-law relationship exists between noise intensity and wind speed so that the log of wind speed may be estimated accurately from spectral ambient noise level by linear least square estimation. At higher frequencies, a non-

linear relationship is expected but we show that it should be possible to make unambiguous low-variance wind speed estimates from broadband noise measurements.

ACKNOWLEDGMENTS

The idea for this work arose during a conversation with Kerry Emanuel of MIT and we thank him for many useful discussions about hurricanes and hurricane classification.

APPENDIX A: NOISE CORRELATION FROM RANDOM SURFACE SOURCES

Previous models for sea-surface noise[5–7] contain approximations or parametrizations that are not valid for the rapidly spatially varying source levels of a hurricane, particularly in the case where the hydrophone is near or under the hurricane. Because of this an alternative expression for calculating the spatial cross-spectral density of the noise field is necessary. The geometry for modeling the spatial cross-spectral density from uncorrelated noise sources at the surface of a stratified ocean waveguide is shown in Fig. 2.

The pressure field created by each surface source is given by the solution to the Helmholtz equation

$$\phi(\mathbf{r},f) = q(\mathbf{r_0},f)g(\mathbf{r}|\mathbf{r_0},f), \tag{A1}$$

where $\phi(\mathbf{r},f)$ is the pressure at $\mathbf{r}$ given a source spectral amplitude $q(\mathbf{r_0},f)$ at $\mathbf{r_0}$ and $g(\mathbf{r}|\mathbf{r_0},f)$ is the waveguide Green function. The total noise field $\phi_S(\mathbf{r},f)$ is the sum of the fields radiated from each source:

$$\phi_S(\mathbf{r},f) = \sum_m^M \phi(\mathbf{r},f) = \sum_m^M q(\mathbf{r_m},f)g(\mathbf{r}|\mathbf{r_m},f). \tag{A2}$$

The spatial correlation of the total field between two receivers $\mathbf{r_1}$ and $\mathbf{r_2}$ can then be written as

$$\begin{aligned} R(\mathbf{r_1},\mathbf{r_2},f',f'') &= \langle \phi_S(\mathbf{r_1},f')\phi_S^*(\mathbf{r_2},f'')\rangle \\ &= \sum_m \sum_n \langle q(\mathbf{r_m},f')q^*(\mathbf{r'_n},f'')\rangle g(\mathbf{r_1}|\mathbf{r_m},f')g^*(\mathbf{r_2}|\mathbf{r_n},f''). \end{aligned} \tag{A3}$$

If the sources have zero mean and are uncorrelated, then $\langle q(\mathbf{r_m},f')q^*(\mathbf{r_n},f'')\rangle = \delta_{m,n}\langle q(\mathbf{r_m},f')q^*(\mathbf{r_n},f'')\rangle$, where $\delta_{m,n}$ is the Kronecker delta function and the correlation simplifies to

$$R(\mathbf{r_1},\mathbf{r_2},f',f'') = \sum_m \langle q(\mathbf{r_m},f')q^*(\mathbf{r_m},f'')\rangle g(\mathbf{r_1}|\mathbf{r_m},f')g^*(\mathbf{r_2}|\mathbf{r_m},f''). \tag{A4}$$

Assuming that the source function q and the received field ϕ_S can be taken to follow a stationary random process in time, at least over the measurement period, then[63] $\langle \phi_S(\mathbf{r_1},f)\phi_S^*(\mathbf{r_2},f')\rangle = C(\mathbf{r_1},\mathbf{r_2},f)\delta(f-f')$ and $\langle q(f)q^*(f')\rangle = S_{qq}(f)\delta(f-f')$ where $S_{qq}(f)$ is the power-spectral density of q and

$$C(\mathbf{r_1},\mathbf{r_2},f) = \sum_m S_{qq}(\mathbf{r_m},f)g(\mathbf{r_1}|\mathbf{r_m},f)g^*(\mathbf{r_2}|\mathbf{r_m},f) \tag{A5}$$

is the cross-spectral density of $\phi_S(\mathbf{r_1})$ and $\phi_S(\mathbf{r_2})$.

For dense source concentrations, this sum can be expressed as an area integral,

$$C(\mathbf{r_1},\mathbf{r_2},f) = \int d^2\boldsymbol{\rho_0} \frac{S_{qq}(\mathbf{r_0},f)}{\Delta A} g(\mathbf{r_1}|\mathbf{r_0},f)g^*(\mathbf{r_2}|\mathbf{r_0},f), \tag{A6}$$

where ΔA is equal to or greater than the coherence area of the random source distribution and corresponds to the smallest differential area summable.

The variance of the source amplitude equals the integrated power spectral density $\langle |q(t)|^2\rangle = \int S_{qq}(f)df$. Since this variance is asymptotically approximated by the sample variance $\langle |q(t)|^2\rangle \approx (1/T)\int_0^T |q(t)|^2\,dt$ for large measurement windows T and since Parseval's theorem has $(1/T)\int_0^T |q(t)|^2\,dt = (1/T)\int_{-\infty}^{\infty} |Q(f)|^2\,df$, we may deduce that

$$S_{qq}(f) \approx \frac{1}{T}|Q(f)|^2, \tag{A7}$$

which relates S_{qq} to practical measurements.

Equation (A6) is similar to an intermediate expression derived by Perkins *et al.* [Eq. (6) of Ref. 7] derived for a significantly different physical scenario as noted in Sec. III. Equation (A6) can be used to model the spatial correlation of the noise field for uncorrelated surface-generated noise when the source distribution or waveguide is range dependent. When the source distribution and environment are range independent, Eq. (A6) reduces to

$$C(\mathbf{r_1},\mathbf{r_2},f) = \frac{2\pi S_{qq}(f)}{\Delta A} \int_{k_r} k_r\,dk_r g(k_r,z_1,z_0)g^*(k_r,z_2,z_0)J_0(k_r|\boldsymbol{\rho_1}-\boldsymbol{\rho_2}|), \tag{A8}$$

following the Kuperman and Ingenito approach[5] where $g(k_r,z_1,z_0)$ is the wavenumber transform of $g(\mathbf{r_1}|\mathbf{r_0},f)$.

APPENDIX B: ASYMPTOTIC VARIANCE FOR WIND SPEED ESTIMATES

The variance of a wind-speed estimate is evaluated numerically in Sec. IV C for some specific scenarios. A general analytic expression is derived here for the asymptotic variance of the wind speed estimate for large sample size μ using Fisher information. For the expected intensity I of an acoustic measurement with a signal-to-noise ratio or time-bandwidth product μ, the inverse Fisher information or Cramer-Rao lower bound (CRLB) of a wind speed estimate $\hat{V}$ is given as[19,64]

$$\mathrm{Var}_{\mathrm{asymptotic}}(\hat{V}) = \left(\frac{\mu}{I^2}\left(\frac{\partial I}{\partial V}\right)^2\right)^{-1}, \tag{B1}$$

which is the asymptotic variance.[63]

At low frequencies the relationship between intensity and wind speed can be expressed using Eq. (22), which, when inserted into Eq. (B1), yields

$$\mathrm{Var}_{\mathrm{asymptotic}}(\hat{V}) = \frac{V^2}{\mu n^2}. \tag{B2}$$

At higher frequencies, where attenuation due to bubbles becomes important, the relationship between intensity and wind speed follows Eq. (19), substituting Eqs. (15), (21), and (23), so that

$$\mathrm{Var}_{\mathrm{asymptotic}}(\hat{V}) = \frac{V^2}{\mu\{n - [VL/(10\log(e))](\partial\alpha/\partial V)\}^2}. \tag{B3}$$

For the attenuation $\alpha(V,f)$ described by Weston[15] in Eq. (4), the CRLB becomes

$$\mathrm{Var}_{\mathrm{asymptotic}}(\hat{V}) = \begin{cases} \dfrac{V^2}{\mu(n - 6.46\times 10^{-7} LV^3\sqrt{f})^2}, & f < 1.5\ \mathrm{kHz}, \\ \dfrac{V^2}{\mu(n - 1.69\times 10^{-8} LV^3 f)^2}, & f > 1.5\ \mathrm{kHz}. \end{cases} \tag{B4}$$

For $V = V_{\max}$ where $V_{\max}$ is given in Eq. (24), the CRLB goes to infinity, indicating that an unbiased estimate of wind speed is not possible for that wind speed and frequency. This problem can be overcome by broadband intensity measurements. For a wind speed estimate given intensity measurements at multiple frequencies, Eq. (B4) becomes

$$\begin{aligned} \mathrm{Var}_{\mathrm{asymptotic}}(\hat{V}) &= \left(\sum_f \frac{\mu(f)}{I(f)^2}\left(\frac{\partial I(f)}{\partial V}\right)^2\right)^{-1} \\ &\approx \begin{cases} \left(\sum_f \dfrac{\mu(f)}{V^2}(n - 6.46\times 10^{-7} LV^3\sqrt{f})^2\right)^{-1}, & f < 1.5\ \mathrm{kHz}, \\ \left(\sum_f \dfrac{\mu(f)}{V^2}(n - 1.69\times 10^{-8} LV^3 f)^2\right)^{-1}, & f > 1.5\ \mathrm{kHz}, \end{cases} \end{aligned} \tag{B5}$$

which remains finite and can be made small by increasing the time-bandwidth product μ.

[1] V. O. Knudsen, R. S. Alford, and J. W. Emling, "Underwater ambient noise," J. Mar. Res. **7**, 410–429 (1948).
[2] G. W. Wenz, "Acoustic ambient noise in the ocean: Spectra and sources," J. Acoust. Soc. Am. **34**, 1936–1956 (1962).
[3] B. F. Cron and C. H. Sherman, "Spatial-correlation functions for various noise models," J. Acoust. Soc. Am. **34**, 1732–1736 (1962).
[4] W. S. Liggett and M. J. Jacobsen, "Covariance of surface-generated noise in a deep ocean," J. Acoust. Soc. Am. **38**, 303–312 (1965).
[5] W. A. Kuperman and F. Ingenito, "Spatial correlation of surface generated noise in a stratified ocean," J. Acoust. Soc. Am. **67**(6), 1988–1996 (1980).
[6] W. M. Carey, R. B. Evans, J. A. Davis, and G. Botseas, "Deep-ocean vertical noise directionality," IEEE J. Ocean. Eng. **15**(4), 324–334 (1990).
[7] J. S. Perkins, W. A. Kuperman, F. Ingenito, L. T. Fialkowski, and J. Glattetre, "Modeling ambient noise in three-dimensional ocean environments," J. Acoust. Soc. Am. **93**, 739–752 (1993).
[8] N. C. Makris, "The statistics of ocean-acoustic ambient noise," in *Sea Surface Sound '97*, edited by T. Leighton (Kluwer Academic, Dordrecht, 1997).
[9] F. Ingenito and S. N. Wolf, "Site dependence of wind-dominated ambient noise in shallow water," J. Acoust. Soc. Am. **85**, 141–145 (1989).
[10] P. T. Shaw, D. R. Watts, and H. T. Rossby, "On the estimation of oceanic wind speed and stress from ambient noise measurements," Deep-Sea Res. **25**, 1225–1233 (1978).
[11] D. L. Evans, D. R. Watts, D. Halpern, and S. Bourassa, "Oceanic winds measured from the seafloor," J. Geophys. Res. **89**(C3), 3457–3461 (1984).
[12] W. M. Carey and D. Browning, "Low frequency ocean ambient noise: Measurements and theory," in *Sea Surface Sound* (Kluwer Academic, Dordrecht, 1988).
[13] A. C. Kibblewhite, "Panel discussion report, wave and turbulence noise," in *Sea Surface Sound* (Kluwer Academic, Dordrecht, 1988).
[14] C. L. Piggott, "Ambient sea noise at low frequencies in shallow water of the Scotian Shelf," J. Acoust. Soc. Am. **36**, 2152–2163 (1964).
[15] D. E. Weston, "On the losses due to storm bubbles in oceanic sound transmission," J. Acoust. Soc. Am. **86**, 1546–1553 (1989).
[16] D. M. Farmer and D. D. Lemon, "The influence of bubbles on ambient noise in the ocean at high wind speeds," J. Phys. Oceanogr. **14**, 1762–1778 (1984).
[17] A. J. Perrone, "Ambient-noise-spectrum levels as a function of water depth," J. Acoust. Soc. Am. **48**, 362–368 (1970).
[18] A. D. Pierce, *Acoustics: An Introduction to Its Physical Principles and Applications* (McGraw-Hill, New York, 1991).
[19] N. C. Makris, "The effect of saturated transmission scintillation on ocean acoustic intensity measurements," J. Acoust. Soc. Am. **100**, 769–783 (1996).
[20] V. F. Dvorak, "Tropical cyclone intensity analysis and forecasting from satellite imagery," Mon. Weather Rev. **103**, 420–430 (1975).
[21] V. F. Dvorak, *Tropical Cyclone Intensity Analysis Using Satellite Data*, NOAA Tech. Rep. NESDIS 11, Washington, DC (1984).
[22] C. S. Velden, T. L. Olander, and R. M. Zehr, "Development of an objective scheme to estimate tropical cyclone intensity from digital geostationary satellite imagery," Weather Forecast. **13**, 172–186 (1998).
[23] J. L. Franklin, L. A. Avila, J. L. Bevin II, M. B. Lawrence, R. J. Pasch, and D. R. Stewart, "Eastern North Pacific hurricane season of 2002," Mon. Weather Rev. **131**, 2379–2393 (2003).
[24] R. J. Pasch, *Tropical Cyclone Report, Hurricane Debby, 19–24 August 2000*, National Hurricane Center, 2000.
[25] J. L. Franklin, *Tropical Cyclone Report, Hurricane Florence, 10–17 September 2000*, National Hurricane Center, 2000.
[26] J. Beven, *Tropical Cyclone Report, Hurricane Keith, 28 September–6 October 2000*, National Hurricane Center, 2000.
[27] L. A. Avila, *Tropical Cyclone Report, Hurricane Iris, 4–9 October 2001*, National Hurricane Center, 2001.
[28] S. R. Stewart, *Tropical Cyclone Report, Hurricane Kyle, 20 September–12 October 2002*, National Hurricane Center, 2002.
[29] R. J. Pasch, *Tropical Cyclone Report, Hurricane Isaac, 21 September–1 October 2000*, National Hurricane Center, 2000.
[30] M. B. Lawrence, *Tropical Cyclone Report, Hurricane Joyce, 25 September–2 October 2000*, National Hurricane Center, 2000.
[31] S. R. Stewart, *Tropical Cyclone Report, Hurricane Michael, 17–19 October 2000*, National Hurricane Center, 2000.
[32] K. B. Katsaros, P. W. Vachon, W. T. Liu, and P. G. Black, "Microwave remote sensing of tropical cyclones from space," J. Phys. Oceanogr. **58**, 137–151 (2002).
[33] G. J. Holland (ed.), *Global Guide to Tropical Cyclone Forecasting* (World Meteorological Organization, Geneva, 1993).
[34] Air Force Reserve Command, Office of Public Affairs, "U. S. air force fact sheet, WC-130 hercules," www.af. mil/factsheets/factsheet.asp?fsID=132
[35] Lt. D. Barr (personal communication, 27 October 2003).
[36] G. J. Holland, "An analytic model of the wind and pressure profiles in hurricanes," Mon. Weather Rev. **108**, 1212–1218 (1980).
[37] K. A. Emanuel, "Thermodynamic control of hurricane intensity," Nature (London) **401**, 665–669 (1999).
[38] R. A. Pielke, Jr. and C. W. Landsea, "Normalized hurricane damages in the U.S.: 1925–1995," Weather Forecast. **13**, 621–631 (1998).
[39] P. J. Hebert, J. D. Jarrell, and M. Mayfield, *The Deadliest, Costliest, and Most Intense United States Hurricanes of this Century (and Other Frequently Requested Hurricane Facts)*, NOAA Tech. Memo., NWS NHC-31, Washington, DC (1993).
[40] G. J. Holland, "The maximum potential intensity of tropical cyclones," J. Atmos. Sci. **54**, 2519–2541 (1997).
[41] R. L. Bankert and P. M. Tag, "An automated method to estimate tropical cyclone intensity using SSM/I imagery," J. Appl. Meteorol. **41**, 461–472 (2002).
[42] C. S. Velden, "Observational analyses of North Atlantic tropical cyclones from NOAA polar-orbiting satellite microwave data," J. Appl. Meteorol. **28**, 59–70 (1989).
[43] S. Q. Kidder, M. D. Goldberg, R. M. Zehr, M. DeMaria, J. F. W. Purdom, C. S. Velden, N. C. Grody, and S. J. Kusselson, "Satellite analysis of

tropical cyclones using the advanced microwave sounding unit (AMSU)," Bull. Am. Meteorol. Soc. **81**(6), 1241–1259 (2000).
[44]Federal Coordinator for Meteorological Services and Supporting Research, *National Hurricane Operations Plan*, U. S. Dept of Commerce/Nat. Oceanic and Atmospheric Administration, FCM-P12-2003 (2003).
[45]P. Ratilal, *Remote Sensing of Submerged Objects and Geomorphology in Continental Shelf Waters with Acoustic Waveguide Scattering*, Ph.D. thesis, Massachusetts Institute of Technology, 2002.
[46]P. Ratilal and N. C. Makris, "Mean and covariance of the forward field propagated through a stratified ocean waveguide with three-dimensional random inhomogeneities," J. Acoust. Soc. Am. (in press).
[47]J. D. Wilson and N. C. Makris, "Full field spatial correlation of range dependent surface generated noise in a stratified ocean with application to hurricane sensing," 143rd Meeting of the Acoustical Society of America, Pittsburgh, PA, June 2002.
[48]R. M. Hamson, "The modeling of ambient noise due to shipping and wind sources in complex environments," Appl. Acoust. **51**(3), 251–287 (1997).
[49]W. J. Pierson and L. Moskowitz, "A proposed spectral form for fully developed wind seas based on the similarity theory of S. A. Kitaigardski," J. Geophys. Res. **69**, 5181–5190 (1964).
[50]D. Hutt, J. Osler, and D. Ellis, "Effect of hurricane Michael on the underwater acoustic environment of the scotian shelf," in *Impact of Littoral Environmental Variability on Acoustic Predictions and Sonar Performance*, edited by N. G. Pace and F. B. Jensen (Kluwer Academic, Dordrecht, Netherlands, 2002).
[51]N. R. Chapman and J. W. Cornish, "Wind dependence of deep ocean ambient noise at low frequencies," J. Acoust. Soc. Am. **93**, 782–789 (1993).
[52]D. H. Cato, "Ambient sea noise in waters near Australia," J. Acoust. Soc. Am. **60**, 320–328 (1976).
[53]V. L. Streeter (ed.), *Handbook of Fluid Dynamics* (McGraw-Hill, New York, 1961).
[54]W. E. Ewing, W. S. Jardetzky, and F. Press, *Elastic Waves in Layered Media* (McGraw-Hill, New York, 1957), pp. 126–130.
[55]S. M. Kay, *Fundamentals of Statistical Signal Processing, Estimation Theory* (Prentice Hall, Englewood Cliffs, NJ, 1993).
[56]R. J. Urick, *Principles of Underwater Sound* (McGraw-Hill, New York, 1983), pp. 57, 389.
[57]C. S. Clay and H. Medwin, *Acoustics Oceanography: Principles & Applications* (Wiley, New York, 1977).
[58]W. S. Burdic, *Underwater Acoustic System Analysis* (Prentice-Hall, Englewood Cliffs, NJ, 1984).
[59]A. J. Perrone, "Deep-ocean ambient-noise spectra in the Northwest Atlantic," J. Acoust. Soc. Am. **3**, 762–770 (1969).
[60]J. A. Nystuen and H. D. Selsor, "Weather classification using passive acoustic drifters," J. Acoust. Soc. Am. **14**, 656–666 (1997).
[61]M. May (personal communication, 15 September, 2004).
[62]*Main Acoustic Clutter Experiment, Initial Report, April 24–May 24*, Office of Naval Research, pp. 53–54.
[63]A. Papoulis and S. U. Pillai, *Probability, Random Variables and Stochastic Processes* (McGraw Hill, Boston, 2002), pp. 513–515, 537–538.
[64]N. C. Makris, "A foundation for logarithmic measures of fluctuating intensity in pattern recognition," Opt. Lett. **20**(19), 2012–2014 (1995).
[65]N. C. Makris, L. Z. Avelino, and R. Menis, "Deterministic reverberation from ocean ridges," J. Acoust. Soc. Am. **97**, 3547–3574 (1995).
[66]S. P. Kumar, T. V. R. Murty, Y. K. Somayajulu, P. V. Chodankar, and C. S. Murty, "Reference sound speed profile and related ray acoustics of Bay of Bengal for tomographic studies," Acustica **80**, 127–137 (1994).
[67]K. D. K. M. Sarma and B. Mathew, "Sound speed structure in the upper layers of equatorial Indian Ocean and Central Bay of Bengal during summer monsoon season," J. Acoust. Soc. India **17**(3-4), 218–221 (1989).
[68]C. Subrahmanyam, N. K. Thakur, T. G. Rao, R. Khanna, M. V. Ramana, and V. Subrahmanyam, "Tectonics of the Bay of Bengal: New insights from satellite-gravity and ship-borne geophysical data," Earth Planet. Sci. Lett. **171**, 237–251 (1999).
[69]E. L. Hamilton, "Geoacoustic modeling of the sea floor," J. Acoust. Soc. Am. **68**, 1313–1340 (1980).
[70]E. L. Hamilton, "Sound velocity as a function of depth in marine sediments," J. Acoust. Soc. Am. **78**, 1348–1355 (1985).
[71]B. E. Tocholke, "Acoustic environment of the Hatteras and Nares Abyssal Plains, Western North Atlantic Ocean, determined from velocities and physical properties of sediment cores," J. Acoust. Soc. Am. **68**, 1376–1390 (1980).